



Study on effect of deposition temperature on photoelectrocatalytic performance of immobilized TiO₂

N.A. Narewadikar, K.Y. Rajpure*

Electrochemical Materials Laboratory, Department of Physics, Shivaji University, Kolhapur 416004, India

ARTICLE INFO

Keywords:

TiO₂
Spray pyrolysis
Photoelectrocatalysis
Organic pollutant
Degradation

ABSTRACT

This work reports the preparation of polycrystalline titanium dioxide (TiO₂) thin films using spray pyrolysis technique at various temperatures to access their photoelectrocatalytic (PEC) performance. The films were characterized by photocurrent response measurements, X-ray diffraction, Scanning electron microscopy, Elemental analysis, Fourier-transform Raman spectroscopy and UV–vis spectroscopy. The TiO₂ showed heterogeneous photocatalytic potential against the oxidative degradation of Phthalic acid (PA) and Benzoic acid (BA) which were used as model pollutants. The PEC behavior of the typical TiO₂ film was excellent for oxidative degradation of both pollutants under UV irradiation.

1. Introduction

The surface and underground water resource management is necessary to ensure continued supply of water for daily use and other activities in the industrial and agricultural sectors. The preservation of water quality is necessary for safe healthy life and sustainable development [1]. The organic pollutants found in waste water such as phenolic compounds [2], polycyclic aromatic hydrocarbons (PAHs) [3] and agricultural chemicals (pesticides and herbicides) are considered as highly toxic and they may lead to the depletion of aquatic system [4]. The organic chemicals discharged into the water bodies are based on hydrocarbons, oxygen and hydroxyl compounds, organometallic compounds etc. Among various waste water purification treatments, the advanced oxidation processes (AOPs) are employed effectively to remove by degradation the organic pollutants from water resources [5–7]. The present study describes the potential use of immobilized titanium dioxide (TiO₂) as photocatalyst for degradation of organic pollutants ubiquitously found in water bodies [8]. TiO₂ powder is extensively investigated for catalytic applications where it is mobile [9,10]. There are limitations to mobile catalysis. Most importantly, it is very tedious to separate catalyst from degraded water after its use. An alternate strategy is to use immobile catalyst which does not remain dissolved in purified water. TiO₂ is mostly used in the environmental protection applications such as air purification and water treatment

[11]. Out of three phases of TiO₂, anatase is most preferred due to its higher adsorption capability and lower recombination rates [12–15]. There are various factors viz. specific surface area, crystallite size, phase of the crystal which affect the photocatalytic performance of TiO₂ [16,17]. Organic pollutants can harm ecosystem stability. Among the different organic pollutants, phthalic acid (PA) and benzoic acid (BA) are used as model organic pollutants in this study. BA [18,19] and PA [20] were selected as organic pollutants as their chemical structures are almost similar and also they are the most common organic pollutants hence making a good choice as model pollutants. Mostly BA comes in wastewater from the pharmaceutical industry whereas PA is mostly released in water bodies from paint industries. Both compounds are toxic and exhibit low biodegradability [21,22]. Therefore, there is need for removal of such harmful organic acids from the water bodies.

This paper presents the results on the preparation of spray deposited TiO₂ thin films at different deposition temperatures. The photoelectrochemical, structural and optical properties of the thin films were studied. The photoelectrocatalytic (PEC) performance of the optimized TiO₂ film was investigated by using PA and BA as the model pollutants. Almost quantitative degradation of the model pollutants was achieved by using the optimized thin film as the photoelectrode. The observations and results presented here highlight the importance of deposition temperatures for obtaining optimum films of TiO₂ and clearly show scientific advancement in thin film based water purification technology.

* Corresponding author.

E-mail address: rajpureky@gmail.com (K.Y. Rajpure).

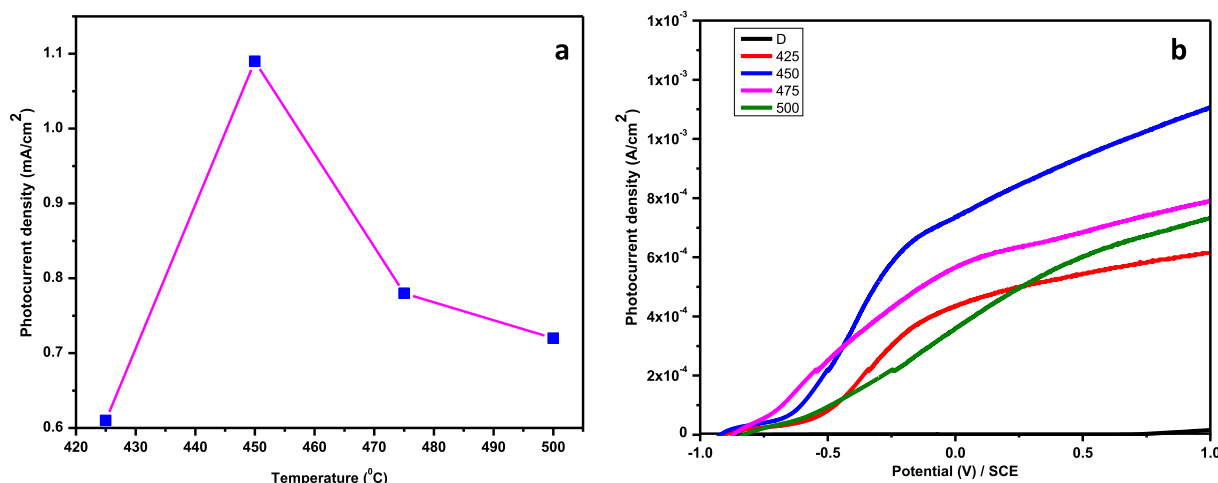


Fig. 1. (a) Variation of I_{ph} with respect to temperature on TiO₂ thin films (b) Current-voltage plot of PEC cell built with TiO₂ ($1 \times 1 \text{ cm}^2$) thin films at 1 V/SCE.

2. Experimental section

2.1. Materials

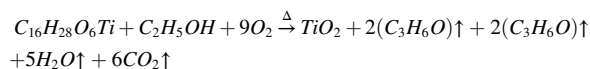
Ti(OPr)₂(acetylacetonate)₂ (Sigma aldrich) was used as Ti source. Ethanol (99.9 % purity), fluorine doped tin oxide (FTO)(15–20 Ω/□ resistivity) with model organic pollutants Phthalic acid and Benzoic acid were purchased from s-d fine chemicals. All chemicals used were of analytical grade and were used as such.

2.2. Methods

2.2.1. Preparation of catalyst.

The ethanolic solution (50 ml) of titanium diisopropoxide bisacetyl acetonate (75 wt%)[TDBA] was used as a Ti precursor. The solution was stirred for 10 min and sprayed over the preheated glass substrates maintained at various temperatures (425 °C –500 °C) in separate sets of experiments with spray rate of 4 cc/min. The obtained films were annealed at 500 °C for 1 h in air atmosphere.

The reaction involved in the formation of TiO₂ thin film is as follows [23]:



The proposed thermal decomposition pathways of TDBA by spray technique is mentioned above. TiO₂ particles are deposited on the glass substrate by evaporation of solvent from precursor and consequently, decomposition of salt into oxides with formation of propylene oxide and propanic acid which gets evaporated. The process results in uniform coating of immobilized TiO₂ thin films on the substrates. The TiO₂ is adhered tightly to the substrate (immobilized) as it is in thin film form. It participates in the photocatalytic reactions in this state and only stays neutral.

2.3. Characterizations of catalyst

The photoelectrocatalytic (PEC) performance of the immobilized TiO₂ film was studied using two electrode system which consists TiO₂ thin film as a photoanode and Platinum as a counter electrode. The crystal structure and phase of the TiO₂ thin films were studied using X-ray diffractometer (Bruker X-ray diffractometer Model D2: phaser with CuK_α radiation of wavelength 1.5406 Å⁰). Scanning electron microscopy (SEM) images were taken on JEOL JSM-6360, Japan instrument for surface morphological analysis. Transmission spectra and absorption spectra of model pollutants at a particular wavelength were recorded

using UV-vis 1800 Spectrophotometer, Shimadzu. Fourier transform Raman spectrometer (Bruker MultiRAM, Germany) with a He-Ne laser source (excitation wavelength of 532 nm) was used to record Raman spectrum within wavenumber range of 100–800 cm⁻¹.

2.4. Testing of phototlectrocatalytic activity

The photo-electrochemical tests were used to investigate the charge separation abilities of samples. The photocurrent response measurements of TiO₂ samples were performed using a Linear sweep voltammetry (LSV) with a power intensity of 20 mW cm⁻² UV irradiation. The scan rate during the measurements was set to be 20 mV s⁻¹ and the electrode area under light irradiation was 1 cm².

Photoelectrocatalytic activity of as synthesized immobilized TiO₂ thin film was investigated for oxidative degradation of PA and BA as model pollutants using single cell reactor. The arrangement of the reactor setup is as discussed in [24] where large area (64 cm²) photo-electrodes were prepared and tested in prototype PEC reactor employing a stainless steel as a counter-electrode and UV tube lamps with $\lambda = 365$ nm.

3. Results and discussion

3.1. Phototlectrocatalytic performance of catalyst

The photoelectrocatalytic performance of spray deposited TiO₂ thin films at different temperatures ranging from 425 °C to 500 °C was studied by plotting a graph of applied potential against photocurrent density at 1 V/SCE. Fig. 1a shows that, as temperature increases, the photocurrent (I_{ph}) starts increasing gradually but later for the films obtained above 450 °C its performance get declined due to formation of stoichiometric TiO₂ thin films with fast charge carrier transfer and the powderish, less compact nature of the film. The photocurrent density for TiO₂ films deposited at 450 °C is maximum. 450 °C deposition temperature is taken to be optimized temperature for film formation as we get more photocurrent for this film. More photocurrent is due to higher photocatalytic efficiency at this deposition temperature. This temperature seems to be appropriate for decomposition and subsequent crystallization of TiO₂. The linear sweep voltammetry (LSV) measurement of TiO₂ films at different temperatures are displayed in Fig. 1b. Here, TiO₂ films deposited at different temperatures did not show the saturation in photocurrent due to more recombination centres where the photocurrent increases non-linearly with respect to applied external bias potential.

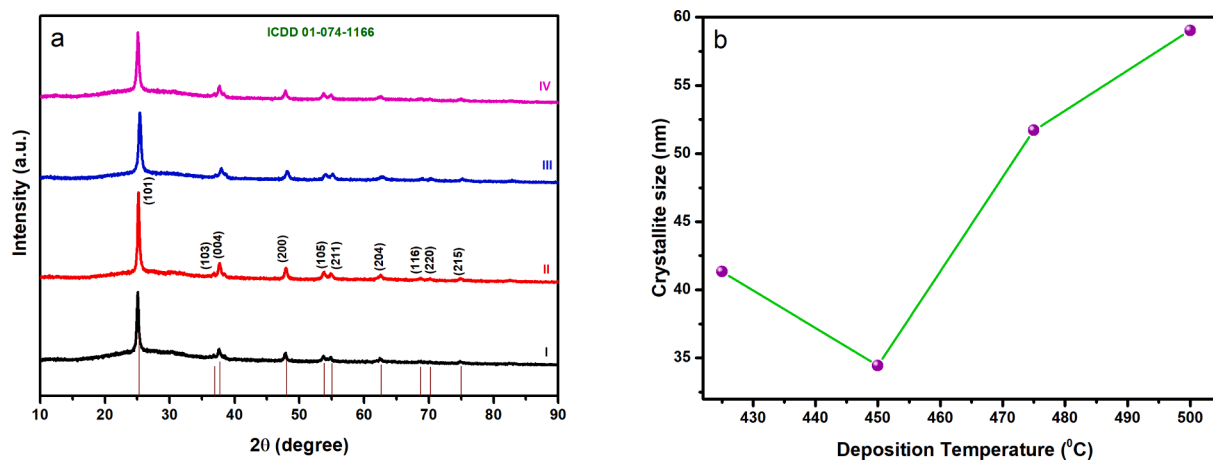


Fig. 2. (a) XRD patterns of spray deposited films at different deposition temperatures (I) 425 °C (II) 450 °C (III) 475 °C (IV) 500 °C. (b) Crystallite size variation with respect to deposition temperatures.

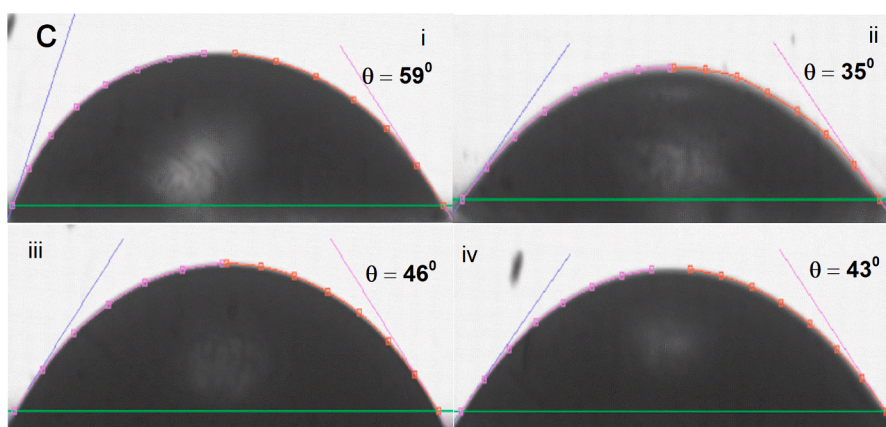
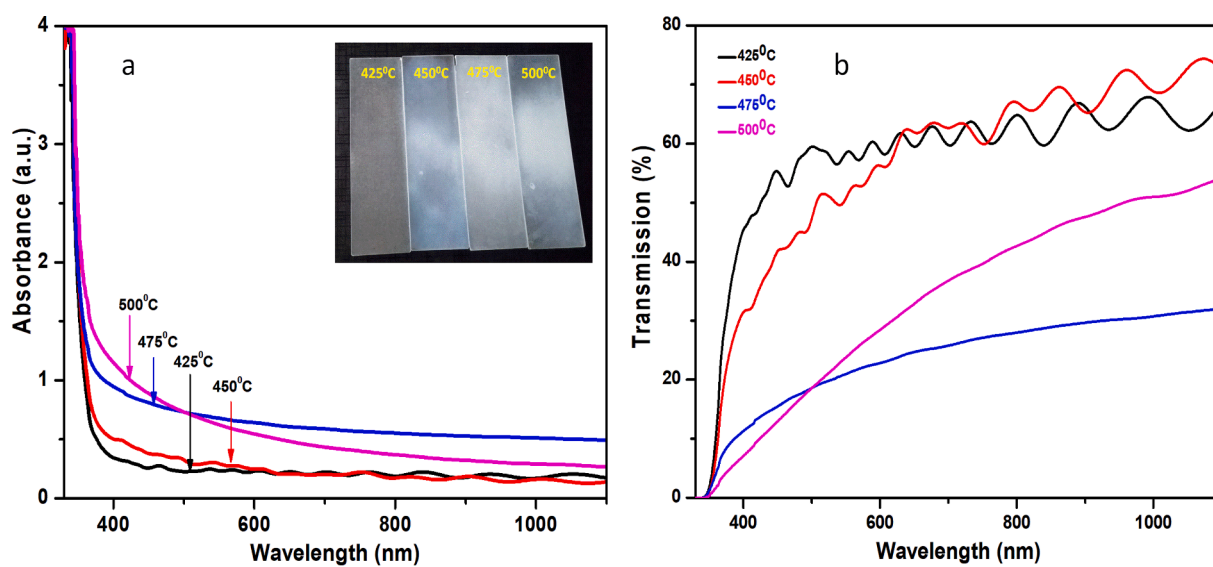


Fig. 3. (a) Plot of variation of absorbance with wavelength of TiO₂ deposited at different temperatures. Inset shows photographs of the samples (b) Transmittance spectra of TiO₂ thin film deposited at various temperatures (c) Water contact angle measurement at (i) 425 °C (ii) 450 °C (iii) 475 °C and (iv) 500 °C.

3.2. Structural analysis: X-ray diffraction

The Fig. 2a shows the X-ray diffraction (XRD) patterns of spray deposited TiO₂ photoelectrodes at different deposition temperatures. The diffraction peaks assigned at different 2θ values as (101), (103),

(004), (200), (105), (211), (204), (116), (220), and (215) planes match with tetragonal anatase phase of TiO₂ (ICDD card no: 01-074-1166). The sharp and intense peaks indicate that the synthesized TiO₂ thin films are highly crystalline. No additional peaks are observed which confirms the pure phase of anatase TiO₂ structure [25]. The anatase

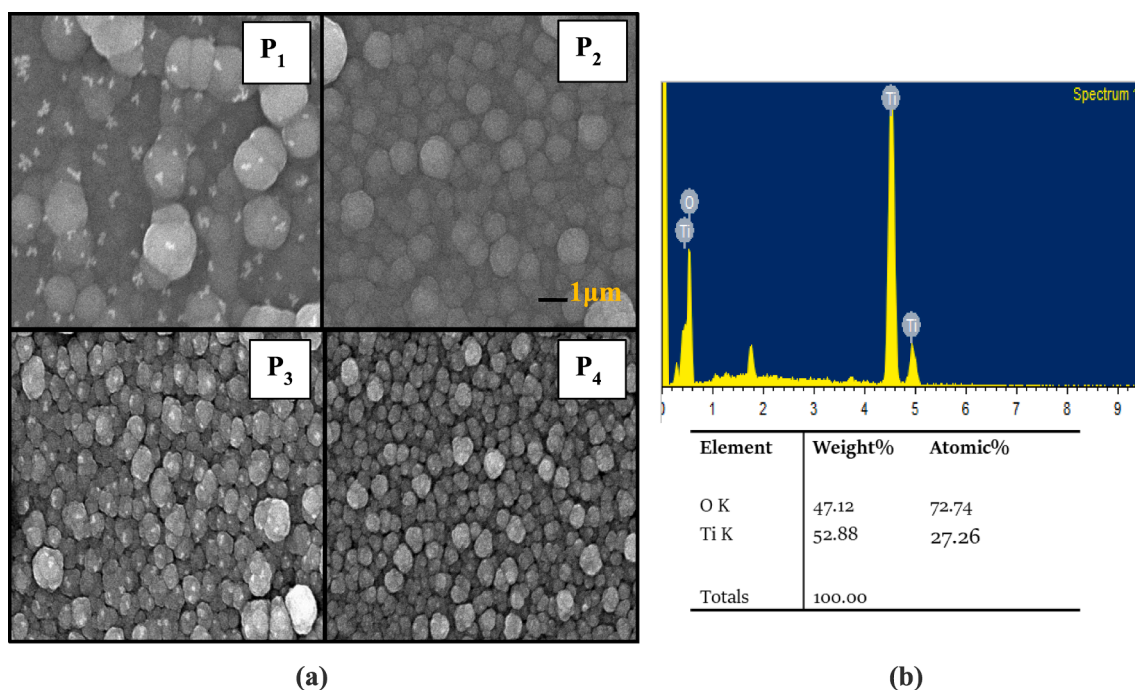


Fig. 4. (a) SEM images of TiO₂ prepared at various temperatures 425 °C, 450 °C, 475 °C, and 500 °C denoted as P₁, P₂, P₃ and P₄ respectively. (b) EDS spectrum of typical sample of TiO₂ film deposited at 450 °C.

phase was further confirmed by Raman spectroscopy. The crystallite size was calculated using Scherer's formula [26]. The variation of crystallite size with respect to temperature is as shown in Fig. 2b, which shows crystallite size varies from 41 to 59 nm. It can be seen that the crystallite size decreases at 450 °C but with further increase in deposition temperature it starts increasing.

3.3. Optical and surface wettability study

The optical absorbance and transmittance spectra (300–1100 nm) of immobilized TiO₂ deposited at different temperatures are shown in Fig. 3. The absorbance spectra (Fig. 3a) showed redshift of band edge with respect to deposition temperature due to powderish appearance of film. Transmittance spectra (Fig. 3b) depict wavy nature of film due to interference and it gets flattened with increasing temperature. The film deposited at 450 °C shows 75% transmittance, further with increase in temperature results in decremented value of transmittance [27]. The photoelectrocatalysis, electromagnetic radiations are illuminated from back contact side. So the catalyst has to be deposited on transparent substrates and it should be more transparent to achieve higher incident photon conversion efficiency (ICPE). Therefore, film deposited at 450 °C is most suitable for achieving higher ICPE and thereby efficient for degradation of organic pollutants undertaking in the present study. Fig. 3c shows water contact angle (CA) images of TiO₂ thin films prepared at various temperatures (425 °C – 500 °C). The observed values of CA vary in the range of 35–59° exhibiting hydrophilic nature of the films. The lower CA was noticed at temperature 450 °C which clearly manifests that pollutant solution stays intact with deposited film for a deferral. This wettability of the film plays a significant role in the photocatalytic degradation of organic pollutants.

3.4. Morphological analysis

The scanning electron microscopy (SEM) images provide information about surface morphology and shape of the particles. Fig. 4a shows SEM micrographs of TiO₂ thin films prepared at various substrate temperatures T_s (425 °C – 500 °C) denoted as P₁, P₂, P₃, P₄ respectively. The

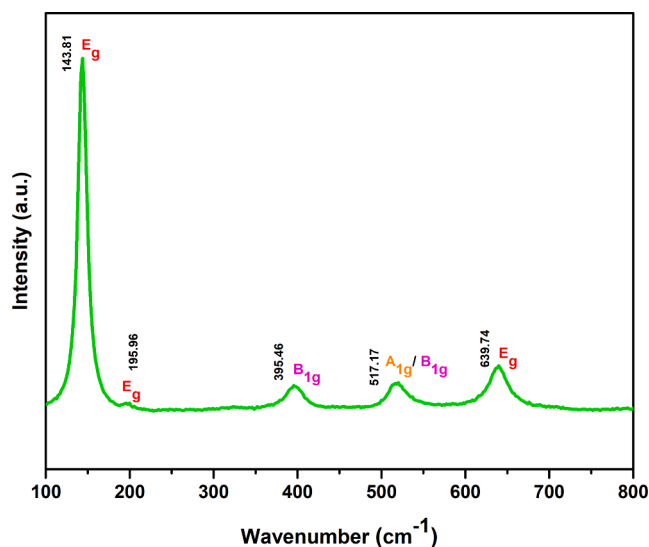


Fig. 5. Raman spectrum of spray deposited TiO₂ prepared at 450 °C.

deposition temperature plays a significant role in the surface morphology of the prepared TiO₂ thin films. It is observed that, with increasing temperature there is increase in the particle size as well as film thickness. The films prepared at T_s = 425–450 °C (Fig. 4a–b) shows smooth grain surfaces where the grains are densely packed due to uniformity and compactness of the particle. The anatase phase formation is kinetically favored at lower temperature [28]. Thus deposition of the films at relatively lower temperatures can give higher surface area, and a higher surface density of active sites for adsorption and catalysis performance [29]. However, when T_s is ≥ 450 °C the grain surfaces become rough and the grains are more loosely packed (Fig. 4a). The increase in the film thickness contributes to the formation of agglomerated clusters in the thin film. The elemental analysis (EDS) result confirmed the purity of the chemically synthesized samples and the data is shown in Fig. 4b.

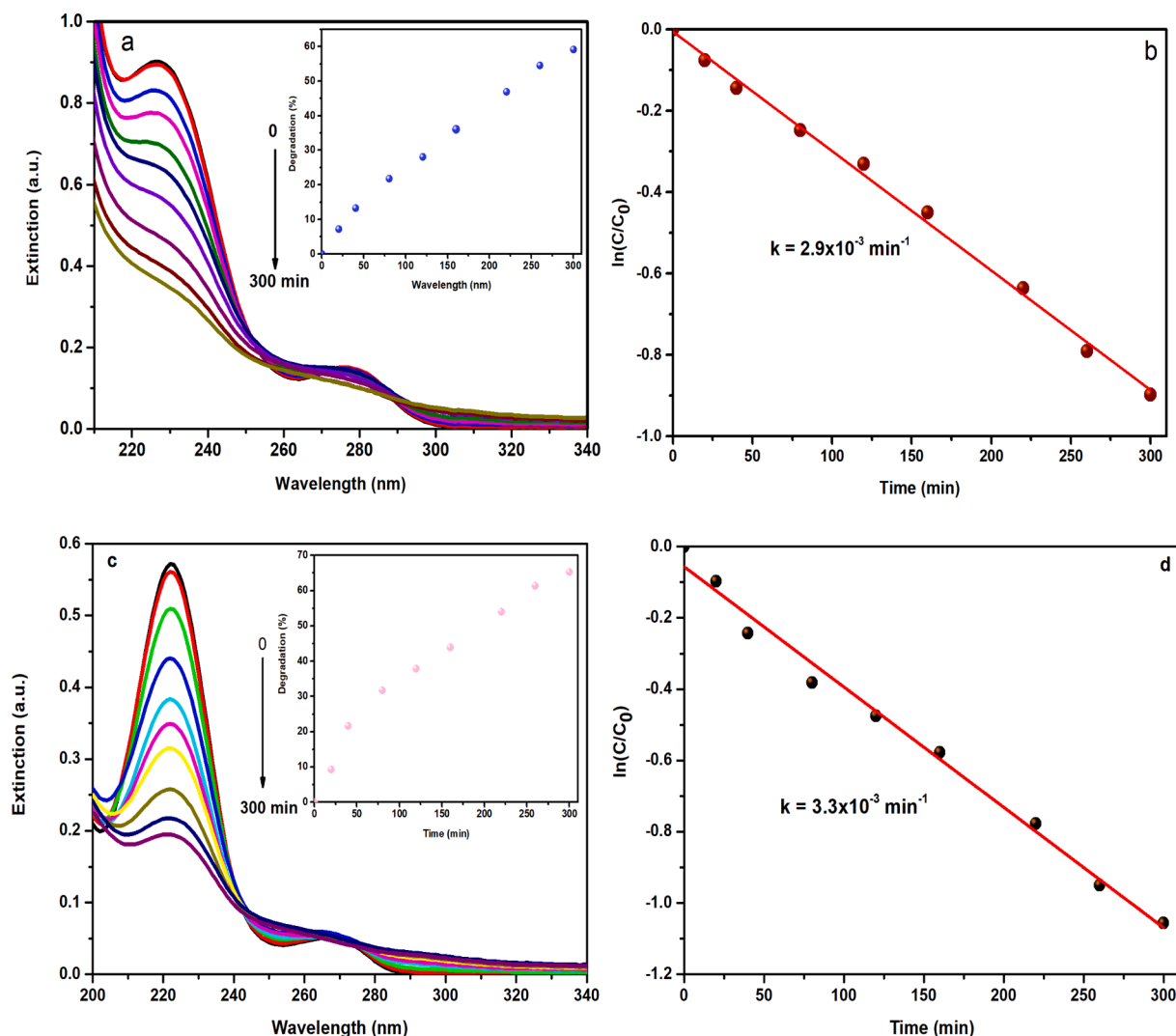


Fig. 6. (a) Degradation of Phthalic acid (PA) using TiO_2 photocatalyst (b) Kinetics of degradation reaction of PA under UV irradiation (c) Degradation of Benzoic acid (BA) using TiO_2 photocatalyst (d) Kinetics of degradation reaction of PA under UV irradiation.

3.5. Raman study

Raman spectroscopy deals with the study of inelastic scattering produced by a molecule. Fig. 5 shows representative Raman spectra of TiO_2 thin film obtained at 450°C . The Raman active mode of anatase phase was shown by six peaks ($A_{1g} + 2B_{2g} + 3E_g$) in Fig. 5 [30,31] with five most intense bands observed for symmetric anatase phase of TiO_2 at $143.8, 195.9, 395.4, 517.1, 639.7\text{ cm}^{-1}$ respectively. The peak centered at 143.8 cm^{-1} defers that the spray deposited TiO_2 film has an anatase phase which is the main characteristics peak of Raman spectrum [32]. The observed data supports the XRD results [33].

3.6. Photoelectrochemical (PEC) measurement

The PEC degradation measurement was performed using a single cell photoreactor with PA and BA being used as model pollutants in separate sets. The minimum concentration of pollutants used was 20 ppm. During the experimentation, TiO_2 was used as anode, and a platinum electrode was used as cathode, 0.5 cm away from anode. The PEC measurements were conducted under 1.5 V bias potential provided by a DC voltage source [34]. The model pollutant solution was circulated through the reactor and the concentration of the pollutant in the solution was monitored by registering the UV visible spectrum at fixed time interval. For the purpose of generation of the main reactive radicals to oxidize

BA/PA in the PEC experiments, PEC degradations of acids with TiO_2 as anode were performed under UV irradiation. The UV light intensity on the surface of samples was measured by luxmeter as 16 mW/cm^2 . Fig. 6a shows the extinction spectrum of PA recorded under UV spectrophotometer shows maximum absorption at 231 nm. The degradation efficiency of the pollutants was examined according to the ratio of C_t and C_0 , where C_t and C_0 are the absorbance of compound in aqueous solution at time t and 0. The degradation efficiency and rate constant are calculated by formula reported earlier [35,36]. The Fig. 6b represents the rate constant $k = 2.9 \times 10^{-3}\text{ min}^{-1}$ due to optimal free radical generation rate. Similarly, the extinction spectrum of BA was recorded using UV spectrophotometer shown in Fig. 6c, which shows peak at 226 nm. Fig. 6d shows logarithmic plot of C/C_0 against time of BA. The slope of this plot gives the rate constant (k), to be $3.3 \times 10^{-3}\text{ min}^{-1}$. The degradation rate in both cases follows first order kinetics with respect to the radiation absorption rate.

Comparing our data with the previous reports [35] there is a possibility of improving or further accelerating the degradation by addition of various oxidants or scavengers as well as increasing the number of PEC cells. It is worth pointing out that here the PEC degradation of organic acids using spray deposited TiO_2 thin films may proceed without producing any harmful byproducts as there is no evolution of absorption maxima observed in the UV visible spectrum registered at each time intervals.

4. Conclusion

In summary, spray deposited immobilized TiO₂ thin films at different temperature were prepared by optimizing the conditions. It is revealed that the deposition temperature significantly affects the crystallinity, morphology of the obtained TiO₂ thin films. The TiO₂ film prepared at 450 °C was found to be more compact in nature, uniform, and with high photocurrent density. The film prepared at 450 °C shows high rate constants for both PA and BA to be $k = 2.9 \times 10^{-3} \text{min}^{-1}$ and $3.3 \times 10^{-3} \text{min}^{-1}$. Therefore the optimized thin film showed effective PEC degradation performance due to its superiority and an effective separation of photogenerated charge carriers in photoelectrocatalytic degradation process that leads to generation of OH radicals which favored the elimination of PA and BA used as model pollutants in the study.

CRedit authorship contribution statement

N.A. Narewadikar: Investigation, Writing – original draft, Writing – review & editing. **K.Y. Rajpure:** Supervision, Writing – review & editing.

Declaration of Competing Interest

The authors declare that they have no known competing financial interests or personal relationships that could have appeared to influence the work reported in this paper.

Acknowledgements

Author N. A. Narewadikar is thankful to Chhatrapati Shahu Maharaj Research Training and Human Development Institute (SARTHI), Pune (India) for financial support through Chhatrapati Shahu Maharaj senior Research Fellowship (CMSRF). This work is partially supported by University Grant Commission (UGC) and Department of Science and Technology (DST), Government of India through providing facilities under DSA-SAP Phase-II and PURSE Phase-II programme at the Department of Physics, Shivaji University Kolhapur, India.

References

- [1] A.A. Azzaz, S. Jellali, N.B.H. Hamed, A. El Jery, L. Khezami, A.A. Assadi, A. Amrane, Photocatalytic treatment of wastewater containing simultaneous organic and inorganic pollution: Competition and operating parameters effects, *Catalysts* 11 (2021) 855, <https://doi.org/10.3390/catal11070855>.
- [2] W.W. Anku, M.A. Mamo, P.P. Govender, Phenolic Compounds in Water: Sources, Reactivity, Toxicity and Treatment Methods, in: M. Soto-Hernández, M. Palma-Tenango, M. del R. Garcia-Mateos (Eds.), *Phenolic Compd. - Nat. Sources Importance Appl.*, InTech, 2017, <https://doi.org/10.5772/66927>.
- [3] H.I. Abdel-Shafy, M.S.M. Mansour, A review on polycyclic aromatic hydrocarbons: Source, environmental impact, effect on human health and remediation, *Egypt. J. Pet.* 25 (1) (2016) 107–123, <https://doi.org/10.1016/j.ejpe.2015.03.011>.
- [4] A. Waheed, Q. Shi, N. Maeda, D.M. Meier, Z. Qin, G. Li, A. Baiker, Strong activity enhancement of the photocatalytic degradation of an azo dye on Au/TiO₂ doped with FeOx, *Catalysts* 10 (2020) 933, <https://doi.org/10.3390/catal10080933>.
- [5] V. Mahmoodi, J. Sargolzaei, Photocatalytic abatement of naphthalene catalyzed by nanosized TiO₂ particles: Assessment of operational parameters, *Theor. Found. Chem. Eng.* 48 (5) (2014) 656–666, <https://doi.org/10.1134/S0040579514050194>.
- [6] S. Hussain, N. Khan, S. Gul, S. Khan, H. Khan, Contamination of Water Resources by Food Dyes and Its Removal Technologies, in: M. Eyvaz, E. Yüksel (Eds.), *Water Chem.*, IntechOpen, 2020. <https://doi.org/10.5772/intechopen.90331>.
- [7] D. Alrousan, A. Afkhami, K. Bani-Melhem, P. Dunlop, Organic degradation potential of real greywater using TiO₂-based advanced oxidation processes, *Water* 12 (2020) 2811, <https://doi.org/10.3390/w12102811>.
- [8] A. Jamil, T.H. Bokhari, T. Javed, R. Mustafa, M. Sajid, S. Noreen, M. Zuber, A. Nazir, M. Iqbal, M.I. Jilani, Photocatalytic degradation of disperse dye Violet-26 using TiO₂ and ZnO nanomaterials and process variable optimization, *J. Mater. Res. Technol.* 9 (1) (2020) 1119–1128, <https://doi.org/10.1016/j.jmrt.2019.11.035>.
- [9] K. Qi, X. Xing, A. Zada, M. Li, Q. Wang, S.-Y. Liu, H. Lin, G. Wang, Transition metal doped ZnO nanoparticles with enhanced photocatalytic and antibacterial performances: Experimental and DFT studies, *Ceram. Int.* 46 (2) (2020) 1494–1502, <https://doi.org/10.1016/j.ceramint.2019.09.116>.

- [10] K. Qi, S.-Y. Liu, M. Qiu, Photocatalytic performance of TiO₂ nanocrystals with/without oxygen defects, *Chin. J. Catal.* 39 (4) (2018) 867–875, [https://doi.org/10.1016/S1872-2067\(17\)62999-1](https://doi.org/10.1016/S1872-2067(17)62999-1).
- [11] Z. Jiang, S. Wickramasinghe, Y.H. Tsai, A.C.S. Samia, D. Gurarie, X. Yu, Modeling and experimental studies on adsorption and photocatalytic performance of nitrogen-doped tio2 prepared via the sol-gel method, *Catalysts* 10 (2020) 1449, <https://doi.org/10.3390/catal10121449>.
- [12] R. Ayouchi, C. Casteleiro, R. Schwarz, J.R. Barrado, F. Martín, Optical properties of TiO₂ thin films prepared by chemical spray pyrolysis from aqueous solutions, *Phys. Status Solidi C*. (2010) NA–NA, <https://doi.org/10.1002/pssc.200982895>.
- [13] M. Okuya, K. Nakade, S. Kaneko, Porous TiO₂ thin films synthesized by a spray pyrolysis deposition (SPD) technique and their application to dye-sensitized solar cells, *Sol. Energy Mater. Sol. Cells*. 70 (4) (2002) 425–435, [https://doi.org/10.1016/S0927-0248\(01\)00033-2](https://doi.org/10.1016/S0927-0248(01)00033-2).
- [14] H. Zhang, Y. Li, W. Li, C. Zhuang, C. Gao, W. Jiang, W. Sun, K. Qi, Z. Sun, X. Han, Designing large-sized cocatalysts for fast charge separation towards highly efficient visible-light-driven hydrogen evolution, *Int. J. Hydrog. Energy*. 46 (56) (2021) 28545–28553, <https://doi.org/10.1016/j.ijhydene.2021.06.134>.
- [15] K. Fischer, A. Gaweł, D. Rosen, M. Krause, A. Abdul Latif, J. Griebel, A. Prager, A. Schulze, Low-temperature synthesis of anatase/rutile/brookite TiO₂ nanoparticles on a polymer membrane for photocatalysis, *Catalysts* 7 (2017) 209, <https://doi.org/10.3390/catal7070209>.
- [16] J. Zhang, P. Zhou, J. Liu, J. Yu, New understanding of the difference of photocatalytic activity among anatase, rutile and brookite TiO₂, *Phys. Chem. Chem. Phys.* 16 (38) (2014) 20382–20386, <https://doi.org/10.1039/C4CP02201G>.
- [17] W. Li, C. Zhuang, Y. Li, C. Gao, W. Jiang, Z. Sun, K. Qi, Anchoring ultra-small TiO₂ quantum dots onto ultra-thin and large-sized Mxene nanosheets for highly efficient photocatalytic water splitting, *Ceram. Int.* 47 (15) (2021) 21769–21776, <https://doi.org/10.1016/j.ceramint.2021.04.192>.
- [18] G. Tekin, G. Ersöz, S. Atalay, Degradation of benzoic acid by advanced oxidation processes in the presence of Fe or Fe-TiO₂ loaded activated carbon derived from walnut shells: A comparative study, *J. Environ. Chem. Eng.* 6 (2) (2018) 1745–1759.
- [19] A.A. Ajmera, S.B. Sawant, V.G. Pangarkar, A.A.C.M. Beenackers, Solar-assisted photocatalytic degradation of benzoic acid using titanium dioxide as a photocatalyst, *Chem. Eng. Technol.* 25 (2002) 173, [https://doi.org/10.1002/1521-4125\(200202\)25:2<173::AID-CEAT173>3.0.CO;2-C](https://doi.org/10.1002/1521-4125(200202)25:2<173::AID-CEAT173>3.0.CO;2-C).
- [20] V.G. Gandhi, M.K. Mishra, P.A. Joshi, A study on deactivation and regeneration of titanium dioxide during photocatalytic degradation of phthalic acid, *J. Ind. Eng. Chem.* 18 (6) (2012) 1902–1907, <https://doi.org/10.1016/j.jiec.2012.05.001>.
- [21] D. Magallanes, J.L. Rodríguez, T. Poznyak, M.A. Valenzuela, L. Lartundo, I. Chairez, Efficient mineralization of benzoic and phthalic acids in water by catalytic ozonation using a nickel oxide catalyst, *New J. Chem.* 39 (10) (2015) 7839–7848, <https://doi.org/10.1039/C5NJ01385B>.
- [22] X. Zhang, C. Zhang, X. Sun, J. Yang, C. Zhu, Mechanism and kinetic study of the reaction of benzoic acid with OH, NO₃ and SO₄^{•-} radicals in the atmosphere, *RSC Adv.* 9 (33) (2019) 18971–18977, <https://doi.org/10.1039/C9RA02457C>.
- [23] I.O. Acik, J. Madarász, M. Krunks, K. Tõnsuaadu, G. Pokol, L. Niinistö, Titanium (IV) acetylacetonate xerogels for processing titania films: A thermoanalytical study, *J. Therm. Anal. Calorim.* 97 (1) (2009) 39–45, <https://doi.org/10.1007/s10973-008-9647-1>.
- [24] N.A. Narewadikar, R.D. Suryavanshi, K.Y. Rajpure, Enhanced photoelectrocatalytic degradation activity of titanium dioxide photoelectrode: Effect of film thickness, *Colloid J.* 83 (1) (2021) 107–115, <https://doi.org/10.1134/S1061933X21010099>.
- [25] K. Qi, R. Selvaraj, T. Al Fahdi, S. Al-Kindy, Y. Kim, G.-C. Wang, C.-W. Tai, M. Sillanpää, Enhanced photocatalytic activity of anatase-TiO₂ nanoparticles by fullerene modification: A theoretical and experimental study, *Appl. Surf. Sci.* 387 (2016) 750–758, <https://doi.org/10.1016/j.apsusc.2016.06.134>.
- [26] I.-L. Hsiao, Y.-J. Huang, Effects of various physicochemical characteristics on the toxicities of ZnO and TiO₂ nanoparticles toward human lung epithelial cells, *Sci. Total Environ.* 409 (7) (2011) 1219–1228, <https://doi.org/10.1016/j.scitotenv.2010.12.033>.
- [27] V. Gopala Krishnan, P. Elango, V. Ganesan, Role of molar concentration in structural, optical and gas sensing performance of anatase phase TiO₂ nanofilms: automated nebulizer spray pyrolysis (ANSP) technique, *Appl. Phys. A*. 123 (2017) 498, <https://doi.org/10.1007/s00339-017-1112-1>.
- [28] R. Dagherir, P. Drogui, D. Robert, Modified TiO₂ for environmental photocatalytic applications: A review, *Ind. Eng. Chem. Res.* 52 (10) (2013) 3581–3599, <https://doi.org/10.1021/ie303468t>.
- [29] J.-M. Herrmann, Heterogeneous photocatalysis: Fundamentals and applications to the removal of various types of aqueous pollutants, *Catal. Today*. 53 (1) (1999) 115–129, [https://doi.org/10.1016/S0920-5861\(99\)00107-8](https://doi.org/10.1016/S0920-5861(99)00107-8).
- [30] G. Cheng, M.S. Akhtar, O.-B. Yang, F.J. Stadler, Structure modification of anatase TiO₂ nanomaterials-based photoanodes for efficient dye-sensitized solar cells, *Electrochimica Acta*. 113 (2013) 527–535, <https://doi.org/10.1016/j.electacta.2013.09.085>.
- [31] E.J. Ekoi, A. Gowen, R. Dorrepaal, D.P. Dowling, Characterisation of titanium oxide layers using Raman spectroscopy and optical profilometry: Influence of oxide properties, *Results Phys.* 12 (2019) 1574–1585, <https://doi.org/10.1016/j.rinp.2019.01.054>.
- [32] L. Wang, T. Qi, J. Wang, S. Zhang, H. Xiao, Y. Ma, Uniform dispersion of cobalt nanoparticles over nonporous TiO₂ with low activation energy for magnesium sulfate recovery in a novel magnesia-based desulfurization process, *J. Hazard. Mater.* 342 (2018) 579–588, <https://doi.org/10.1016/j.jhazmat.2017.08.080>.
- [33] A.G. Ilie, M. Scarisoareanu, I. Morjan, E. Dutu, M. Badiceanu, I. Mihailescu, Principal component analysis of Raman spectra for TiO₂ nanoparticle

- characterization, *Appl. Surf. Sci.* 417 (2017) 93–103, <https://doi.org/10.1016/j.apsusc.2017.01.193>.
- [34] S. Shajari, E. Kowsari, N. Seifvand, F. Boorboor Ajdari, A. Chinnappan, S. Ramakrishna, G. Saianand, M. Dashti Najafi, V. Haddadi-Asl, S. Abdpour, Efficient photocatalytic degradation of gaseous benzene and toluene over novel hybrid PIL@TiO₂/m-GO composites, *Catalysts* 11 (2021) 126, <https://doi.org/10.3390/catal11010126>.
- [35] Y.M. Hunge, A.A. Yadav, V.L. Mathe, Oxidative degradation of phthalic acid using TiO₂ photocatalyst, *J. Mater. Sci. Mater. Electron.* 29 (8) (2018) 6183–6187, <https://doi.org/10.1007/s10854-018-8593-3>.
- [36] V.S. Mohite, M.A. Mahadik, S.S. Kumbhar, Y.M. Hunge, J.H. Kim, A.V. Moholkar, K.Y. Rajpure, C.H. Bhosale, Photoelectrocatalytic degradation of benzoic acid using Au doped TiO₂ thin films, *J. Photochem. Photobiol. B.* 142 (2015) 204–211, <https://doi.org/10.1016/j.jphotobiol.2014.12.004>.